Journal of Alloys and Compounds 509 (2011) 7267–7270

Contents lists available at ScienceDirect

Journal of Alloys and Compounds

journal homepage: www.elsevier.com/locate/jallcom

In doped ZnO thin films

A. Hafdallah, F. Yanineb, M.S. Aida*, N. Attaf

Laboratory of Thin Films and Interface, Faculty of Science, Department of Physics, University Mentouri of Constantine 25000, Algeria

ARTICLE INFO

Article history:
Received 21 December 2010
Received in revised form 11 April 2011
Accepted 11 April 2011
Available online 20 April 2011

Keywords:
ZnO
Thin films
Ultrasonic spray
Semiconductor doping

ABSTRACT

ZnO thin films were deposited by ultrasonic spray technique, zinc acetate was used as starting solution with a molarity of 0.1 M. A set of indium (In) doped ZnO (between 2 and 8 wt%) thin films were grown on glass substrate at 350 °C. The present work is focused on the influence of the doping level on the structural, optical and electrical films properties. Optical film characterization was carried by using UV–visible transmission spectroscopy, the optical gap was deduced from absorption. From X ray diffraction (XRD) analysis, we have deduced that ZnO films are formed with nanocrystalline structure with preferential (0 0 2) orientation. The grain size is increased with In doping from 28 to 37 nm. Electrical characterization was achieved using two-probes coplanar structure, the measured conductivity varies from 2.3 to 5.9 $\Omega\,cm^{-1}$ when increasing the doping level. However the optical gap is reduced from 3.4 to 3.1 eV.

1. Introduction

ZnO thin films became the most promising candidate material for the production of optoelectronic devices in the UV region and optical or display devices. They are used as gas sensors [1], surface acoustic devices [2], transparent electrodes [3] and solar cells [4,5]. Zinc oxide has a wide band gap of 3.3 eV, low resistivity and high transparency in the visible range.

ZnO thin films have been mainly prepared by numerous methods such as: sputtering [6,7], chemical vapour deposition [8,9], sol–gel process [10,11] and spray pyrolysis [12–17]. Spray pyrolysis technique is attractive because it is simple, efficient and non contaminating production process [18]. It is based on the spray of droplets produced from Zn containing solution on a heated substrate. Droplets are generated by two ways: (i) the solution containing the precursors is carried by a relatively pressurized air flow, the atomization into droplets is formed at the nozzle orifice. This method is called the pneumatic spray (PS); (ii) the solution is atomized by an ultrasonic wave generator, this is so-called ultrasonic spray (USP). The droplet size is more uniform and finer in ultrasonic spray jet than in pneumatic spray. Moreover, the droplet velocity is relatively low in USP than in PS, these differences may have an influence in films growth in these two methods. The PS technique is largely used by comparison to USP one. On the other hand, ZnO thin films have been prepared by many researchers using an aqueous solution with and without adding alcohol [19–21]. However, only a few studies have dealt with the deposition of ZnO in non aqueous medium.

ZnO can be doped with a wide variety of ions. The ZnO doping is achieved by replacing Zn^{2+} atoms with atoms of elements of higher valance such as In^{3+}, Al^{3+}, Sn^{4+} and Pb^{4+}. Several deposition techniques are used to grow indium doped zinc oxide (IZO) thin films such as: sputtering [22–24], sol gel [25] and spray pyrolysis [26–31]. For IZO films prepared by spray pyrolysis, the In introduction into film network was achieved by adding indium chloride (InCl) into the zinc salt solution [26–30], or by ZnO spraying on a substrate with In evaporated layer and followed by a subsequent annealing [28]. However, only a few studies have been devoted to the influence of In doping level and the investigated doping ratio In/Zn do not exceed 5 wt% [30].

In the present study, we have investigated the effect of a larger In doping ratio range (up to 8%) on the structural, optical and electrical properties of indium doped zinc oxide thin films deposited by ultrasonic spray. Moreover, ZnO thin films were deposited by ultrasonic spray technique with a non aqueous starting solution.

2. Experimental

The samples used in this study were deposited using a home made system. The starting solution is composed with 0.1 molarity of zinc acetate ($C_4H_6O_4Zn{\cdot}2H_2O$) salt diluted in methanol. In doping is achieved by adding a small quantity of $InCl_3$ in the solution. The weight of the added dopant source is calculated as function of the desired In/Zn ratio. The latter was varied in the range of 0–8%. The prepared solution is then sprayed on the heated glass substrates by ultrasonic nebulizer system (Sonics) which transforms the liquid to a stream formed with uniform and fine droplets of 40 μm average diameter (given by the manufacturer). The temperature of the substrates was 350 °C.

---

* Corresponding author.
E-mail address: aida_salah2@yahoo.fr (M.S. Aida).

0925-8388/$ – see front matter © 2011 Elsevier B.V. All rights reserved.
doi:10.1016/j.jallcom.2011.04.058

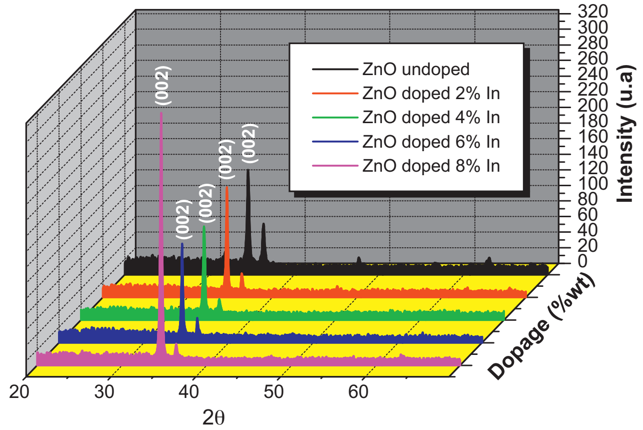

Fig. 1. X-ray diffraction spectra of undoped and In doped ZnO thin films.

The structural characterization of the films was carried out by X-ray diffraction technique using an X-ray diffractometer (Philips X'Pert) with CuKα radiation. The grain size is simply determined using the Scherrer formula:

$$D = \frac{0.9\lambda}{\beta \cos\theta}$$

where D is the grain size of crystallite, λ (=1.54059 Å) the wavelength of X-rays used, β the broadening of diffraction line measured at half of its maximum intensity and θ is the angle of diffraction.

The films' optical transmittances were studied by using Shimadzu 3101 PC UV–visible spectrophotometer. The thickness of the film was calculated using the following relation:

$$d = \frac{\lambda_1\lambda_2}{2(n_1\lambda_2 - n_2\lambda_1)}$$

where n_1 and n_2 are the refractive indices at the two adjacent maxima (or minima) at λ_1 and λ_2. The zinc oxide film thickness was found to be 0.25 μm.

The measured films thicknesses of our films were between 250 nm and 300 nm.

The absorption coefficient α of ZnO films was determined from transmittance measurements. The films' absorption coefficient was calculated using the following expression:

$$\alpha = -\frac{1}{d}\ln T$$

where T is the normalized transmittance and d is the film thickness. These absorption coefficient values were used to determine optical energy gap. The energy gap (E_g) was estimated by assuming a direct transition between valence and conduction bands from the expression:

$$(\alpha h\nu)^r = \beta(h\nu - E_g)$$

where β is a constant, the exponent r is equal to 2 and 1/2 for direct allowed and indirect allowed transitions respectively. Since ZnO is known to be a direct semiconductor we have chosen the exponent $r = 2$.

E_g is determined by extrapolating the straight line portion of the spectrum to $\alpha h\nu = 0$.

The absorption coefficient of films shows a tail for sub-bandgap photon energy this tail is so-called Urbach tail. The latter, which is closely related to the disorder in the film network, is expressed as [15].

$$\alpha = \alpha_0 \exp\left(\frac{h\nu}{E_u}\right)$$

where α_0 is a constant and E_u is the Urbach energy.

The electrical conductivity of the films was measured in a coplanar structure obtained with evaporation of two golden stripes on film surface.

3. Results and discussion

3.1. Structural properties

Fig. 1 shows the XRD patterns of undoped and In doped films with different doping levels. As seen from this figure, the films exhibit a dominant peak at $2\theta = 34.34°$ corresponding to the (0 0 2) plane of ZnO. Other peaks corresponding to (1 0 0) and (1 0 1) plans are also present in the spectra indicating the polycrystalline nature of the obtained films.

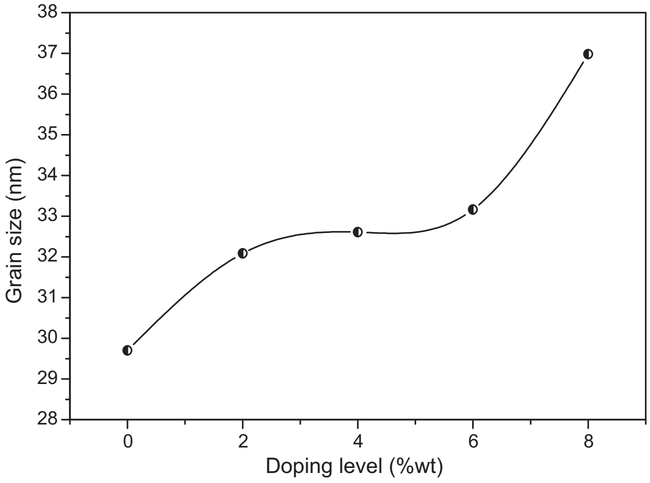

Fig. 2. Variation of grain size with doping level.

It is also evident in Fig. 1 that the preferential (0 0 2) peak intensity increases with increasing In dopant concentration. This indicates an improvement in films crystallinity with In film doping. This is due to the fact that the In incorporation in film network enables more nucleation sites. However, in contrary to In doped ZnO thin films prepared by pneumatic spray (PS) [27], the films' crystallinity is degraded [30] with In doping and the preferential orientation are changed from [0 0 2] to (1 0 1) and (1 0 0) [26,29]. This discrepancy may be due to the difference in the surface reactions involved during film growth in both techniques.

No new phases have been observed in the XRD pattern even at higher doping level. Thereafter, the In incorporation does not alter the hexagonal structure of ZnO films and does not initiate the formation of In_2O_3 phase. The same conclusion has been reported by Ratheesh Kumar et al. in ZnO thin film doped by evaporation of In layer followed by annealing [28].

Fig. 2 shows the variation of the grain size calculated from the XRD pattern as mentioned in Section 2. The grain size increases with increasing the doping level. This is a general trend observed by many authors [27,31].

3.2. Optical properties

Fig. 3 shows the optical transmission spectra recorded in the range from 200 to 800 nm obtained in films prepared with different In doping levels. As can be seen, a region of strong transparency is located between 400 and 800 nm. The value of the transmission is about 65–85%. In this wavelength range we have also observed interference fringes. These fringes are due to the multiple reflections on the two interfaces of the film. This indicates that the films prepared with these conditions are smooth and uniform [12]. In addition, a strong absorption region, which corresponds to the fundamental absorption due to the inter-band electronic transition, is seen in the higher photon energy region.

The optical gap and the Urbach tail energy are estimated from the absorption coefficient variation, as described in Section 2. Fig. 4a and b shows a typical variation of $(\alpha h\nu)^2$ and $\ln\alpha$ drawn as a function of photon energy respectively. Fig. 4a is used to extrapolate the optical band gap, while Fig. 4b is used to deduce the Urbach band tail width. Fig. 5 shows the variations of the optical gap together with the Urbach tail energy as a function of In doping level. It is clear that the optical gap is reduced with In doping. This band gap narrowing is due to the increase in the band tail width as shown

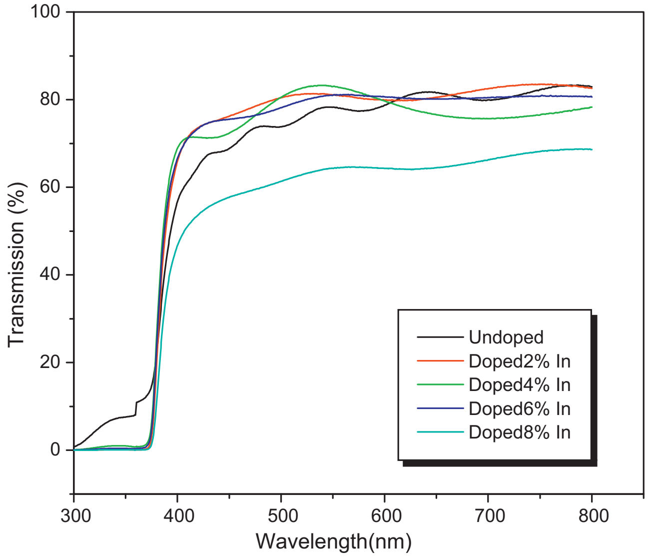

Fig. 3. Transmission spectra of undoped and In doped ZnO thin films.

in Fig. 5. It is worth to bear in mind that the Urbach tail energy is closely related to the disorder in the film network. Since the ion radius of In is larger than Zn [27], the In introduction into the film is then followed by the lattice distortion and consequently disorder creation which cause the optical reduction. The same conclusion has been reported by Paul et al. [34] in Zr doped ZnO and Ilican et al. [30] in In doped ZnO prepared by PS spray.

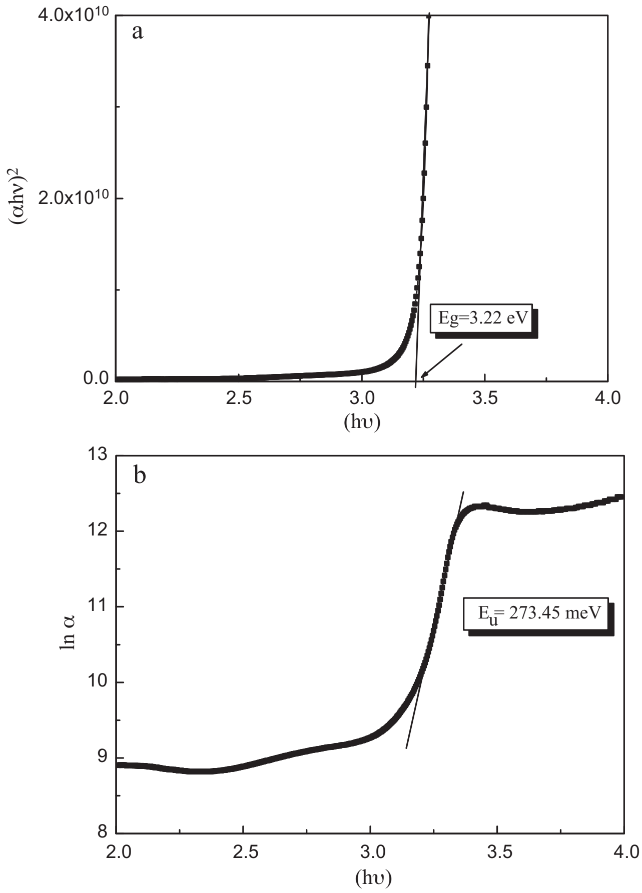

Fig. 4. Typical variation of: $(\alpha h\nu)^2$ and $\ln\alpha$ drawn as a function of photon energy used respectively for: (a) optical band gap and (b) Urbach tail width determination

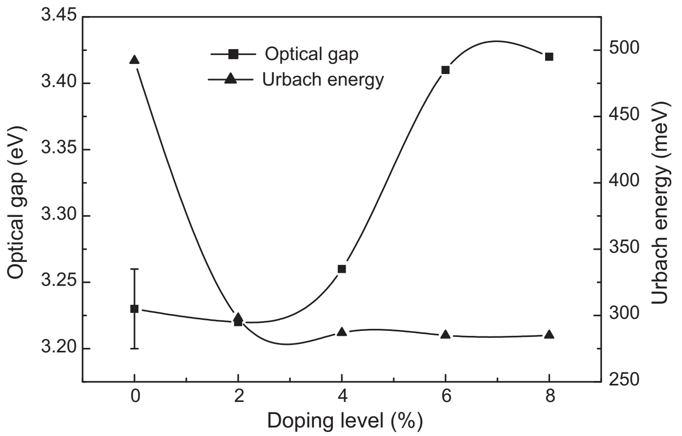

Fig. 5. Variation of optical band gap and Urbach energy with doping level.

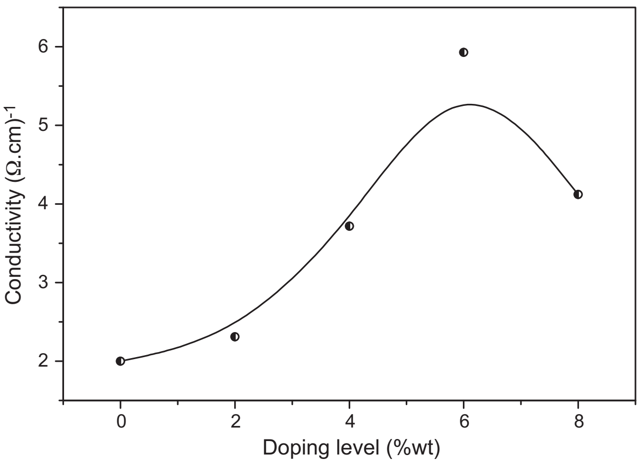

Fig. 6. Electrical conductivity of undoped and In doped ZnO thin films.

3.3. Electrical properties

Fig. 6 shows the variation of the conductivity of In doped ZnO thin films. The obtained results indicate that the conductivity of the samples increases with the increase in doping level and reached its maximum value of 5.3 $\Omega\,\mathrm{cm}^{-1}$ with a concentration of indium of 6%. This increase in conductivity with the increase in the In concentration can be attributed to the increase in the free carriers (electrons) concentrations. The latter are coming from the ions In^{3+} donors in the substitutional sites of Zn^{2+} [12]. The electrical conductivity increases with doping level up to 6% (Fig. 6). With further increase of In ratio the conductivity is reduced. The same behavior was reported by many authors in In doped ZnO thin films [29,31], Al doped ZnO thin films [31–33] and Zr doped ZnO [34]. The reduction in the conductivity is due to the inactivity of added dopant atoms. However the doping ratio threshold of the conductivity diminution was ranged from 0.8% for Al to 2% for In and Zr doping which is lower than our case. The reduction of the conductivity with increasing the doping level is explained by the feature that the excess of introduced atoms are segregated into the grain boundaries where they become electrically inactive [23].

4. Conclusions

ZnO thin films were deposited by ultrasonic spray technique with a non aqueous solution. The effect of In concentration on the structural, optical and electrical properties of films was investigated. The crystallinity of doped films is improved with In doping. Doped ZnO films preserve their (0 0 2) preferential orientation. The optical gap is reduced with the increase in doping ratio because of the disorder introduction with incorporation In the film network. The electrical conductivity is enhanced with In doping suggesting that introduced In atoms act as donors. However, doping beyond 6% is followed by the conductivity reduction.

References

[1] H. Xu, X. Liu, D. Cui, M. Li, M. Jiang, Sens. Actuators B: Chem. 114 (2006) 301.
[2] W. Water, S.-Y. Chu, Y.-D. Juang, S.-J. Wu, Mater. Lett. 57 (2002) 998.
[3] D.R. Sahu, S.-Y. Lin, J.-L. Huang, Appl. Surf. Sci. 252 (2006) 7509.
[4] J.B. Yoo, A.L. Fahrenbruch, R.H. Bube, J. Appl. Phys. 68 (1990) 4694.
[5] J.B. Baxter, E.S. Aydil, Sol. Energy Mater. Sol. Cells 90 (2006) 607.
[6] K.H. Kim, K.C. Park, D.Y. Ma, J. Appl. Phys. 81 (1997) 7764.
[7] M. Miyazaki, M. Sato, K. Mitsui, H. Nishimura, J. Non-Cryst. Solids 218 (1997) 323.
[8] M. Puica, E. Budano, E. Rusu, M. Danila, R. Gavrila, Thin Solid Films 3404 (2002) 485.
[9] N.D. Kumar, M.N. Kamalasanan, S. Chandra, Appl. Phys. Lett. 65 (1994) 1373.
[10] D. Bao, H. Gu, A. Kuang, Thin Solid Films 312 (1998) 37.
[11] Z.M. Jarzebeski, Phys. Stat. Solidi 71 (1982) 13.
[12] S.A. Studenikin, N. Golego, M. Cocivera, J. Appl. Phys. 83 (1998) 2104.
[13] R. Ayouchi, D. Leinen, F. Martin, M. Gabas, E. Dalchiele, J.R. Ramos-Barrado, Thin Solid Films 426 (2003) 68.
[14] P. Nunes, B. Fernandes, E. Fortunato, P. Vilarinho, R. Martins, Thin Solid Films 337 (1999) 176.
[15] F. Paraguay, W. Estrada, D.R. Acosta, E. Andrade, M. Miki-Yoshida, Thin Solid Films 350 (1999) 192.
[16] M.N. Islam, M.O. Hakim, H. Rahman, J. Mater. Sci. 22 (1987) 1379.
[17] S. Major, A. Banerjee, K.L. Chopra, Thin Solid Films 108 (1983) 333.
[18] E. Lopez-Navarette, M. Ocana, J. Eur. Ceram. Soc. 22 (2002) 313.
[19] C. Zhang, X. Li, J. Bian, W. Yu, X. Gao, Solid State Commun. 132 (2004) 75.
[20] J.H. Lee, B. Park, Mater. Sci. Eng. B 106 (2004) 242.
[21] J. Bian, X. Li, L. Chen, Q. Yao, Chem. Phys. Lett. 393 (2004) 256.
[22] D.Y. Ku, I.H. Kim, I. Lee, K.S. Lee, T.S. Lee, J.H. Jeong, B. Cheong, Y.-J. Baik, W.M. Kim, Thin Solid Films 350 (2006) 192.
[23] K.H. Kim, K.C. Park, D.Y. Ma, J. Appl. Phys. 81 (1997) 15.
[24] P. Sagar, M. Kumar, R.M. Mehra, Mater. Sci. 23 (2005) 3.
[25] G. Srinivasan, J. Kumar, J. Cryst. Growth 310 (2008) 1841.
[26] S. Ilican, Y. Caglar, M. Caglar, F. Yakuphanoglu, Physica E 35 (2006) 131–138.
[27] Y. Caglar, S. Ilican, M. Caglar, F. Yakuphanoglu, Spectrochim. Acta A 67 (2007) 1113.
[28] P.M. Ratheesh Kumar, C. Sudha Kartha, K.P. Vijayakumar, J. Appl. Phys. 98 (2005) 023509.
[29] D.J. Goyal, C. Agashe, M.G. Takwale, V.G. Bhide, J. Mater. Res. 8 (1993) 5.
[30] S. Ilican, Y. Caglar, M. Caglar, B. Demirci, J. Optoelectron. Adv. Mater. 10 (2008) 2592–2598.
[31] P. Nunes, E. Fortunato, P. Tonillo, F.B. Fernández, P. Vilarinho, R. Martins, Vacuum 64 (2002) 281–285.
[32] S.B. Majumder, M. Jain, P.S. Dobal, R.S. Katiyar, Mater. Sci. Eng. B 103 (2003) 16–25.
[33] A.F. Aktaruzzaman, G.L. Sharma, L.K. Malhotra, Thin Solid Films 198 (1991) 67.
[34] G.K. Paul, S. Bandyopadhyay, S.K. Sen, S. Sen, Mater. Chem. Phys. 79 (2003) 71.